The Prostate Dot Engine – a System-Guided and Assisted Workflow to Improve Consistency in Prostate MR Exams

Wilhelm Horger, Gregor Thoermer, Elisabeth Weiland, Bernd Kuehn, Berthold Kiefer

Siemens Healthineers, Magnetic Resonance Imaging, Erlangen, Germany

The "PROMISe" of mpMRI

PROMIS, PRECISION, 4M and MRI-FIRST [1–4] are four landmark studies that are changing the way we screen for prostate cancer.

Evidence presented in these studies has already impacted guidelines on imaging prostate cancer issued by the European Association of Urology and national guidelines in the UK (NICE) and the Netherlands toward a scheme where prostate MRI serves a first-line triage test in biopsy-naïve men with elevated PSA levels.

These studies consistently provide Level 1A evidence that using multiparametric MRI (mpMRI) of the prostate can reduce the number of biopsies required in men with elevated PSA levels.

Due to the excellent negative predictive value of prostate mpMRI, men without suspicious MRI findings do not require further examinations. At the same time, the mpMRI pathway does not result in an under-detection of clinically significant cancer, but will reduce the number of clinically insignificant cancers picked up by chance in a "systematic TRUS-biopsy-only" care scheme (see Table 1). It has been shown for – quite differently organized – healthcare systems that the MRI pathway will reduce the overall healthcare expenditure per clinically significant cancer diagnosed. This advantage is largely driven by the reduced number of biopsies [5–7], resulting in fewer infections and sepsis, the latter presenting a huge financial burden [8]. The potential long-term effects on patient management of reduced detection of clinically insignificant disease have not even been modelled in studies of this kind.

Performance of mpMRI pathway in comparison with TRUS-bx pathway	PRECISION[1] (500 men)	MRI-FIRST[2]	4M Study[3]	PROMIS[4]
Avoid biopsy after negative mpMRI in (%) of patients	28 %	18 – 21 %	49 %	27 %
Increase in detection of significant cancers (%)	+12 %	No difference in significant cancer (+2 %)	No difference in significant cancer (+2 %)	No difference in significant cancer (+2 %)
Diagnosis of insignificant cancer	-13 %	-14 %	-11 %	-5 %
Reduction of biopsy cores per patient (relevant for infections and side effects	11 → 4 (= -64 %)	12 → 3 (= -75 %)	12 → 3 (= -75 %)	n.a.

Table 1: Summary of recently published landmark mpMRI prostate cancer detection studies and their impact on patient management.

The challenge in scaling up mpMRI

Expert panels are, however, aware that the MRI pathway puts an additional burden on radiologists and imaging providers and the potential risks and challenges associated with the increasing demand. Most radiologists have limited expertise in interpreting and reporting prostate MRI, and the consistent acquisition of high-quality mpMRI prostate examinations is a challenge for technologists not used to performing the exam routinely according to the PI-RADS recommendations.

In 2019, Engels et al. [9] and Barrett et al. [10] published excellent papers on how to perform high-quality mpMRI and which pitfalls to consider. They concluded that training of skilled professionals is key; but also that imaging vendors should provide tools and workflows that help tailor and optimize the exam for the individual patient, to maximize scan quality and consistency.

Respective software automatically detecting characteristic landmarks with machine learning trained algorithms to adjust size and angulation of FOVs to the individual anatomical conditions with high consistency and reproducibility has been successfully established for various applications, literarily ranging from head to toe with the Brain, Spine, Hip, Knee, Breast, Cardiac, Abdomen, and Whole-Body Dot Engines. Studies specifically investigating the value of such software for assisted and guided brain, liver and whole-body examinations have clearly shown relevant reduction of examination time compared to standard workflows [11–13]. In addition, for liver examinations, assisting features including automated bolus detection (ABLE) with an automatically positioned bolus tracker in the descending aorta allow technologists to achieve optimal arterial phase quality in dynamic contrast-enhanced scans in 94% of cases, where a fixed-time approach only achieves 73% of optimally timed arterial phase images [12].

Prostate Dot Engine[1] – from prototype to product

Such novel automated scanner software has recently been prototyped and evaluated for MRI examinations of the prostate. The aim is to standardize scan volume positioning, tilting and coverage, in order to ensure high consistency between operators, and to better support Active Surveillance with repeated MR scans [14]. Although the evaluation did not show a statistically significant time advantage of the assisted workflow over the manual workflow (26 versus 28 minutes median examination time), the overall imaging quality was superior with the assisted MRI scans, achieving an average rating of 4.6 out of 5 versus 3.8 out of 5 points for the manual workflow.

In the light of developing evidence and changing guidelines, the planned introduction of the Prostate Dot Engine as part of the software version *syngo* MR XA30A is timely.

The Prostate Dot Engine is designed for fast, reproducible and standardized prostate MR examinations and supports multi-parametric, multi-plane MR imaging according to the latest PI-RADS v2.1 recommendations [15]. The operator is guided through one comprehensive workflow with decision points to adapt the strategy to individual patient conditions (see Figure 1), while artificial intelligence aids in planning and performing the procedure steps.

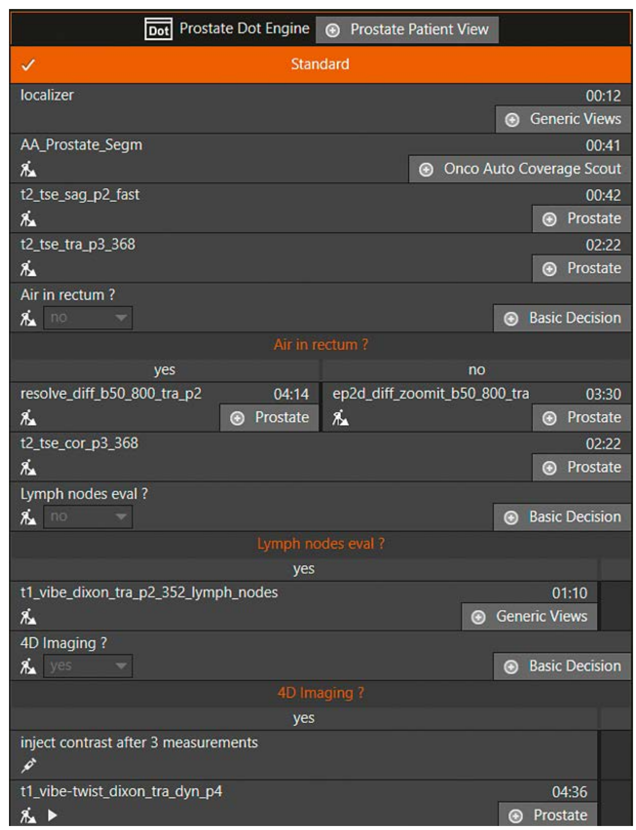

1 Workflow of the Prostate Dot Engine with different decision points.
For example, based on initial morphological scans the operator may be asked to decide whether a patient has a lot of gas in the rectum. If there is considerable gas, a highly robust RESOLVE DWI scan is acquired. If not, zoomed diffusion-weighed images are acquired. These are more prone to distortions, but offer higher spatial resolution and better contrast in shorter time.

[1] Work in progress: the product is currently under development and is not for sale in the U.S. and in other countries. Its future availability cannot be ensured.

AI-assisted planning, angulation, and coverage

Before image acquisition, the operator has the choice between two general approaches for acquiring the data. In "Patient View" (Fig. 2) slice orientation can be chosen to be either "Anatomical" or "Axial". Anatomical means that the acquisition volumes are tilted to match the actual, individual angulation of the prostate in the body, which can be affected by factors such as bladder and rectal filling, or how the patient lies on the bed. Most recommendations and committees suggest acquiring either axial scans "perpendicular to the long axis of the prostate" or "true axial" images, the latter aimed at improving reproducibility in Active Surveillance [9, 15, 16].

A recent study has investigated the robustness of AI-derived axial slice angulation with the Prostate Dot Engine. Subjects underwent MRI scans of the prostate with full and empty bladder, with excellent reproducibility of the angulation [17], indicating that the assisted planning approach might increase consistency in Active Surveillance without compromising fidelity in anatomical coverage. The preferred angulation strategy can be predefined and set as a default, so it does not have to be selected in every patient.

The short AutoAlign prostate segmentation scan at the beginning of the exam facilitates the detection of certain landmarks in the small pelvis to derive the angulation and coverage required for the subsequent mpMRI of the prostate. For the angulation, the entry point of the bladder neck into the prostate and the exit of the urethra from the apex of the prostate are used as highly reproducible landmarks. In addition, the prostate gland is automatically segmented, and if the PSA value has been specified an estimate of PSA density (ng/ml) is provided in the generated report. Another feature of the Prostate Dot Engine is to support asymmetric anatomical coverage or a shift in the field-of-view direction as illustrated in Figure 3.

By default, images in the sagittal plane are acquired before the axial T2-weighted and diffusion-weighted images. This approach has repeatedly been reported to be beneficial as it gives the patient some time to relax and calm down, so they are less likely to move during the most relevant axial scans.

Diffusion-weighted imaging

After acquiring T2-weighted images in sagittal and transverse orientation, diffusion-weighted images are automatically pre-planned and acquired, using either RESOLVE or a

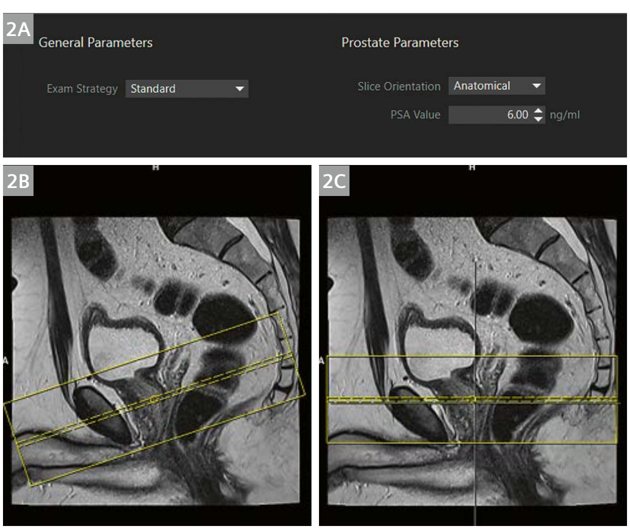

2 The Patient View of the Prostate Dot Engine **(2A)** is displayed before the examination. The operator can specify the desired slice orientation ("Anatomical" or "Axial"), which will result in the acquisition orientations shown in **2B** and **2C**, respectively. Coronal and sagittal acquisitions are acquired perpendicular to the chosen axial orientation. The PSA value can be entered in order to get an automated estimation of the PSA density.

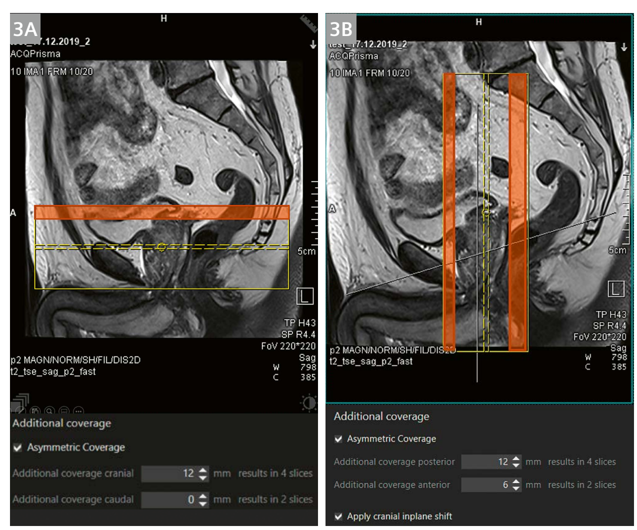

3 Based on the segmentation of the prostate gland, the required number of slices to cover the entire organ is automatically derived and adjusted. In particular with straight axial acquisitions, the seminal vesicles may expand more in the cranial direction than the prostate base **(3A)**. To ensure complete coverage of the seminal vesicles, the user interface allows to specify additional "asymmetric coverage", for example with 4 more slices in the cranial direction (corresponding to the orange area). The same can also be applied to other orientiations, e.g., to coronal planes **(3B)**. In addition, a FOV shift to better cover lymph nodes in the small pelvis can be achieved by ticking the option "Apply cranial inplane shift" thus ending the FOV 5 cm below the apex of the prostate.

single-shot EPI method with reduced FOV (ZOOMit^PRO^). The strengths of both techniques are specified in Table 2 and an illustrative case can be found in Figure 4.

Following the PI-RADS v2.1 recommendation, two *b*-values (b = 50 s/mm^2 and b = 800 s/mm^2) are scanned and ultra-high *b*-value images at b = 1400 s/mm^2 are automatically calculated. The often-suggested additional acquisition of a supporting *b*-value in the range of 400–500 s/mm^2 for improved ADC calculation is not recommended here, since a linear fitted ADC value is hardly influenced by this choice and the scan time may more effectively be invested in additional averages at the higher *b*-value.

With regards to the ultra-high *b*-value (> 1400 s/mm^2) there is some disagreement in the international community whether to acquire or extrapolate images, and on the optimal choice of the ultra-high *b*-value [18]. UK consensus guidelines are most specific in proposing b ≥ 1400 s/mm^2 at 1.5T and b ≥ 2000 s/mm^2 at 3T, both "preferentially acquired". Rosenkrantz et al. [20] provide some guidance on the choice of an optimal *b*-value, suggesting that "computed *b*-values in the range of 1500–2500 s/mm^2 (but not higher) are optimal for prostate cancer detection" providing high sensitivity for lesions and sufficient anatomical clarity.

The Prostate Dot Engine provides a flexible framework where protocol steps can be modified and added to best serve individual institutional expectations.

Dynamic contrast-enhanced imaging

After acquiring diffusion-weighted and coronal T2-weighted images, T1-weighted scans of the small pelvis and dynamic contrast-enhanced (DCE) images may be acquired. Some studies [20, 21] suggest that the detection rate of clinically significant cancer may not be negatively affected with a bi-parametric screening protocol, but the detection rate of insignificant cancer and the number of biopsies may go up due to a tendency to upgrade indecisive cases without DCE information. On the other hand, bi-parametric protocols have the clear advantage of being completely non-invasive and substantially shorter, there-

	ZOOMit^{Pro}	RESOLVE
TE (ms)	72	51
FOV (mm x mm)	100 x 100	200 x 200
Resolution (mm^3)	0.82 x 0.82 x 3.0	0.85 x 0.85 x 3.0
Acquisition time (min:sec)	3:30	4:14

Table 2: Comparison of protocol parameters of ZOOMit^{Pro} and RESOLVE with b = 50, 800 s/mm^2 at 3T (MAGNETOM Prisma). While ZOOMit provides higher SNR and resolution in shorter acquisition time, the readout segmented RESOLVE is more robust in patients with susceptibility issues (especially caused by gas in rectum) due to a substantially shorter echo train.

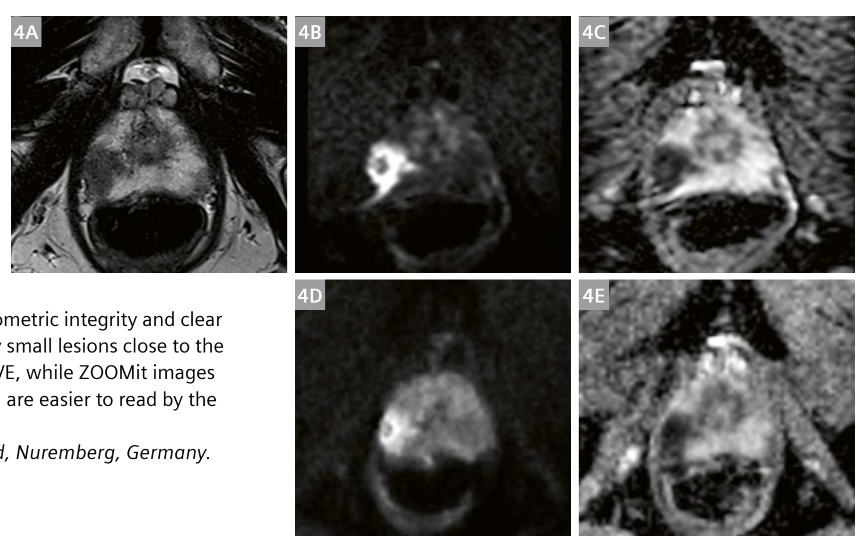

4 72-year-old patient with suspected prostate cancer. A clearly visible lesion in the right periperal zone in the apical aspect of the prostate **(4A)** represented with a corresponding diffusion restriction in calculated high *b*-value images and ADC maps. Due to a substantial amount of gas in the rectum, ZOOMit images **(4B, D)** suffer from a distortion in phase-encoding-direction (here: L-R), sometimes also referred to as "comet tail sign" while the RESOLVE images **(4C, E)** expose high geometric integrity and clear lesion delineation. It can be argued that very small lesions close to the capsule may only be seen properly in RESOLVE, while ZOOMit images appear to have higher lesion conspicuity and are easier to read by the radiologists.
Images courtesy of Prof. Karlheinz Engelhard, Nuremberg, Germany.

fore more cost efficient. While the role of DCE in prostate cancer detection is debated and may be subject to change in a later version of PI-RADS, DCE remains integral part of PI-RADS v2.1 conform mpMRI for now. This is also reflected in the workflow of the Prostate Dot Engine: by default, DCE imaging is included but may be deselected (i.e. in follow-ups) or removed if this is the institutional preference. As for the other scans, positioning of the imaging volume is automatically adjusted and imaging parameters, such as temporal and spatial resolution, are kept constant to fulfill the requirements of the PI-RADS standard.

Summary

The Prostate Dot Engine aims to standardize mpMRI of the prostate, to assist less experienced users in performing the scans with consistent high quality, and to facilitate high reproducibility in repeated scans, for example in Active Surveillance. The Prostate Dot Engine is one of several intelligent solutions designed to scale up prostate MRI in the light of a globally rising demand for this procedure.

References

1 Kasivisvanathan V, Rannikko AS, Borghi M, et al. PRECISION Study Group Collaborators. MRI-Targeted or Standard Biopsy for Prostate-Cancer Diagnosis. N Engl J Med. 2018;378(19):1767-1777.
2 Rouvière O, Puech P, Renard-Penna R, et al. Use of prostate systematic and targeted biopsy on the basis of multiparametric MRI in biopsy-naive patients (MRI-FIRST): a prospective, multicentre, paired diagnostic study. Lancet Oncol 2018; http://dx.doi.org/10.1016/S1470-2045(18)30569-2.
3 van der Leesta M, Cornelb E, Israëla B, et al. Head-to-head comparison of transrectal ultrasound guided prostate biopsy versus multi-parametric prostate resonance imaging with subsequent MR-guided biopsy in biopsy-naïve men with elevated PSA; a large prospective multicenter clinical study. Eur Urol. 2018; in press.
4 Ahmed HU, El-Shater Bosaily A, Brown LC, et al. Diagnostic accuracy of multi-parametric MRI and TRUS biopsy in prostate cancer (PROMIS): a paired validating confirmatory study. Lancet. 2017;389: 815–22.
5 de Rooij M, Crienen S, Witjes JA, et al. Cost-effectiveness of magnetic resonance (MR) imaging and MR-guided targeted biopsy versus systematic transrectal ultrasound-guided biopsy in diagnosing prostate cancer: a modelling study from a health care perspective. Eur Urol. 2014;66(3):430-436.
6 Pahwa S, Schlitz NK, Ponsky LE, et al. Cost-effectiveness of MR Imaging-guided Strategies for Detection of Prostate Cancer in Biopsy-Naive Men. Radiology. 2017;285(1):157-166.
7 Faria R, Soares MO, Spackman E, et al. Optimising the Diagnosis of Prostate Cancer in the Era of Multiparametric Magnetic Resonance Imaging: A Cost-effectiveness Analysis Based on the Prostate MR Imaging Study (PROMIS). Eur Urol. 2018;73(1):23-30. doi: 10.1016/j.eururo.2017.08.018. Epub 2017 Sep 19.
8 Gross MD, Alshak MN, Shoag JE, et al. Healthcare Costs of Post-Prostate Biopsy Sepsis. Urology. 2019;133:11-15.
9 Engels RRM, Israël B, Padhani AR, et al. Multiparametric Magnetic Resonance Imaging for the Detection of Clinically Significant Prostate Cancer: What Urologists Need to Know. Part 1: Acquisition. Eur Urol. 2019 in press; DOI: https://doi.org/10.1016/j.eururo.2019.09.021.
10 Caglic I, Barrett T. Optimising prostate mpMRI: prepare for success. Clin Radiol. 2019 ;74(11):831-840.
11 Moenninghoff C, Umutlu L, Kloeters C, et al. Workflow efficiency of two 1.5T MR scanners with and without an automated user interface for head examinations. Acad Radiol. 2013;20(6):721-30.
12 Sharma P, Kalb B, Kitajima HD, et al. Optimization of single injection liver arterial phase gadolinium enhanced MRI using bolus track real-time imaging. J Magn Reson Imaging. 2011;33(1):110-8.
13 Stocker D, Finkenstaedt T, Kuehn B, et al. Performance of an Automated Versus a Manual Whole-Body Magnetic Resonance Imaging Workflow. Invest Radiol. 2018;53(8):463-471.
14 Esser M, Zinsser D, Kündel M, et al. Performance of an Automated Workflow for Magnetic Resonance Imaging of the Prostate: Comparison With a Manual Workflow. Invest Radiol. 2019. doi: 10.1097/RLI.0000000000000635
15 American College of Radiology. PI-RADS® Prostate Imaging – Reporting and Data System 2019, Version 2.1. https://www.acr.org/-/media/ACR/Files/RADS/Pi-RADS/PIRADS-V2-1.pdf
16 Appayya MB, Adshead J, Ahmed HU. National implementation of multi-parametric magnetic resonance imaging for prostate cancer detection – recommendations from a UK consensus meeting. https://doi.org/10.1111/bju.14361.
17 Cui Y, Han S, Li C, et al. Performance and Reproducibility of a Day Optimizing Throughput (Dot) Workflow Engine in Automated Prostate MRI Positioning. Proceedings of the 28th Annual Meeting of the ISMRM, Abstract No. #4546.
18 Kordbacheh H, Seethamraju RT, Harisinghani MG, et al. Image quality and diagnostic accuracy of complex-averaged high b value images in diffusion-weighted MRI of prostate cancer. Abdominal Radiology. 2019 June;44(6):2244-2253.
19 Brizmohun AM, Adshead J, Ahmed HU, et al. National implementation of multi-parametric magnetic resonance imaging for prostate cancer detection – recommendations from a UK consensus meeting. BJU Int. 2018;122:13-25. https://doi.org/10.1111/bju.14361.
20 Rosenkrantz AB, Parikh N, Kierans AS, et al. Prostate Cancer Detection Using Computed Very High b-value Diffusion-weighted Imaging: How High Should We Go? Acad Radiol. 2016;23(6):704-11.
21 Kuhl CK, Bruhn R, Krämer N, et al. Abbreviated Biparametric Prostate MR Imaging in Men with Elevated Prostate-specific Antigen. Radiology. 2017;285(2):493-505.
22 Van der Leest M, Israël B, Cornel EB, et al. High Diagnostic Performance of Short Magnetic Resonance Imaging Protocols for Prostate Cancer Detection in Biopsy-naïve Men: The Next Step in Magnetic Resonance Imaging Accessibility. Eur Urol. 2019;76(5):574-581.

Contact

Wilhelm Horger
MR Application Development
Siemens Healthineers
wilhelm.horger@siemens-healthineers.com